Longitudinal Power Profile Estimation in WDM Transmission and Optical Network Tomography

Inwoong Kim
Fujitsu Network Communications, Inc.
Richardson, USA
inwoong.kim@fujitsu.com

Olga Vassilieva
Fujitsu Network Communications, Inc.
Richardson, USA
olga.vassilieva@fujitsu.com

Ryu Shinzaki
Fujitsu Limited
Kawasaki, Japan
shinzaki.ryu@fujitsu.com

Motohiko Eto
Fujitsu Limited
Kawasaki, Japan
eto.motohiko@fujitsu.com

Shoichiro Oda
Fujitsu Limited
Kawasaki, Japan
oda.shoichiro@fujitsu.com

Paparao Palacharla
Fujitsu Network Communications, Inc.
Richardson, USA
paparao.palacharla@fujitsu.com

***Abstract*—We evaluate longitudinal power profile estimator based on coherent receiver in WDM configurations and identify the impact of nonlinear rotation of constellation caused by copropagating neighboring channels. We also review prototype of optical tomography.**

Keywords—optical network tomography, optical link monitoring, coherent optical communications

I. Introduction

As optical networks evolve toward autonomous and desegregated networks, optical transmission link monitoring became important. Especially, longitudinal power profile estimation (PPE) in nonlinear optical transmission link based on coherent receiver draw interests because it measures power profile in multi-spans without any additional hardware compared to OTDR (optical time domain reflectometer) [1]. The application of PPE has been shown for anomaly loss detection in multi-span transmission, band-pass profile estimation, gain profile characterization in EDFA/Raman hybrid transmission links, and longitudinal power profile in Raman links, PDL monitoring and so on [1-5].

Nonlinear and dispersion process in optical fiber is not commute such that the received waveform is uniquely determined by the accumulation history of distributed nonlinear interference noise and dispersion along the transmission line, which enables PPE because nonlinear interference noise contribution at any point in optical fiber is proportional to signal power at the location. There are two major branches of PPE based on coherent receiver. One is correlation-based method (Correlation-PPE) and the other one is minimum mean square-error based method (MMSE-PPE) [6,7]. In both methods, two waveforms are compared. One is reference waveform at the receiver and the other one is emulated waveform transmitted from transmitter. In emulation, MMSE-PPE emulate nonlinear propagation based on multi-step split-step Fourier method (or Volterra-based nonlinear propagation) while Correlation-PPE performs single-step split-step method. First PPE was demonstrated based on Correlation-PPE [1]. Then, many different MMSE-PPEs have been reported such as neural network based digital backpropagation and Volterra nonlinear equalizer, linear least square methods [3,4].

In determining power profile, MMSE-PPE minimizes the difference of electrical field of waveforms while Correlation-PPE evaluates correlation between intensity of waveforms. These differences between two methods bring pros and cons. MMSE-PPE shows better spatial resolution with absolute power profile compared to Correlation-PPE [6,7]. But MMSE-PPE needs to know nonlinear rotation θ_{nl} of constellation in transmission line (Fig. 1) or needs separate algorithm for estimation of θ_{nl}. Correlation-PPE is comparing intensity of waveforms such that it can work without knowing nonlinear rotation of constellation. We reported in [8] that it is hard to measure θ_{nl} in practical system because of random linear phase noise from environmental perturbation on fiber and finite laser linewidth. In addition, θ_{nl} and random linear phase noise are removed by CPR (carrier phase recovery) in coherent receiver. We proposed SF-MMSE-PPE (MMSE-PPE with complex *scaling factor*) that performs MMSE-PPE with automatic adjustment of constellation rotation [8]. SF-MMSE-PPE showed robust performance than C-MMSE-PPE (conventional MMSE-PPE) for unknown θ_{nl} [8].

We further identify that it is not easy to measure θ_{nl} in WDM configurations even in ideal simulation study. In this paper, we show that the impact of unknown nonlinear rotation of constellation in WDM transmission configuration on correlation-PPE, C-MMSE-PPE, and SF-MMSE-PPE. We also review recently demonstrated optical network tomography, anomaly detection and fiber type identification, in experimental testbed for optical networks.

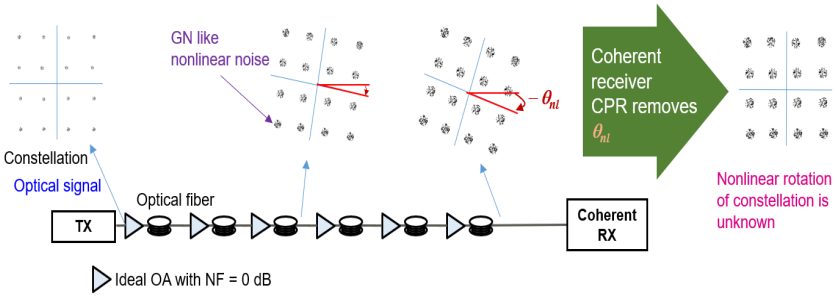

Fig. 1. Schematic diagram explaining nonlinear rotation (θ_{nl}) of constellation in ideal optical transmission link without ASE noise, any environmental perturbation or laser phase noise. CPR compensates nonlinear rotation.

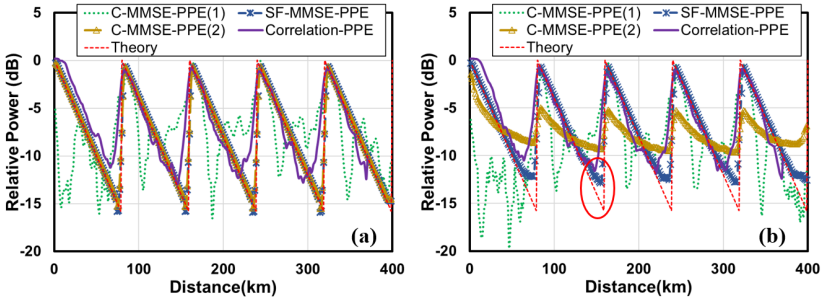

Fig. 2. Estimated longitudinal power profile depending on PPE methods. 'Theory' is calculated based on transmission distance, span length and fiber attenuation. (a) single channel transmission, (b) 3-WDM channel transmission.

II. Impact of Nonlinear Rotation of Constellation In WDM Transmission

Fig. 1 shows how the constellation rotates due to fiber nonlinearity as optical signal propagates along the optical transmission links. In general, Gaussian-like noise caused by nonlinear interference in optical fiber contributes to transmission impairment, but nonlinear rotation is not considered in GN model because this can be easily compensated by CPR for symbol decision in coherent receiver. But this factor should be considered for emulation of signal propagation in nonlinear optical fiber for MMSE-PPE.

To understand the impact of WDM transmission configuration on MMSE-PPE, we compare two different transmission configurations. A single channel or three channels of Nyquist pulse shaped 96 Gbaud DP-16QAM is/are transmitted where channel spacing is set as 125 GHz. The transmission link has 5 spans of 80 km SMF where fiber dispersion is 17 ps/nm/km, nonlinear coefficient is 1.3 /W/km, and fiber attenuation is 0.2 dB/km. No ASE noise is added, and the sampled data (2 samples/symbol) is saved assuming ideal coherent receiver (no laser phase noise with zero linewidth). 20 different data patterns of 2^{14} symbols are transmitted (2^{19} symbols for Correlation-PPE). Estimated power profiles by PPE are averaged for evaluation of performance. Three different PPEs are evaluated: Correlation-PPE, C-MMSE-PPE, and SF-MMSE-PPE.

There are two different options in PPE: (1) CPR is performed at the receiver side such that nonlinear rotation is removed, (2) CPR is not performed that received waveform keeps the nonlinear rotation θ_{nl}. Fig. 2 (a) shows the estimated power profile when a single channel is transmitted depending on PPE. Correlation-PPE does not estimate exact relative power profiles such that estimated profile is scaled properly and down-slope matches with fiber attenuation profile. Correlation-PPE shows the same results without regards to two different options. SF-MMSE-PPE also shows consistent estimation without regards to the options as expected. SF-MMSE-PPE shows better performance, almost overlapped with theoretical estimation, compared to Correlation-PPE. C-MMSE-PPE shows comparable performance to SF-MMSE-PPE if option (2) is used. However, C-MMSE-PPE may fail to estimate power profile when option (1) is chosen. Fig. 2 (b) shows the estimated power profile when WDM channels are transmitted. SF-MMSE-PPE shows the expected power profile comparable to theoretical estimation without regards to options. The mismatch near the low power region of optical signal in fiber (marked with red circle) might be contributed to additional nonlinear noise from neighboring channels, cross-phase modulation, that is not considered in MMSE-PPE. Correlation-PPE also showed comparable estimation of power profile without regards to options. However, C-MMSE-PPE fails for both options. Especially, it fails even for the option where nonlinear rotation of constellation is preserved in received waveform without CPR. The reason is that the received waveform has the nonlinear rotation of constellation caused by total power in fiber or power of 3 channels while nonlinear rotation of constellation caused by the evaluation channel only should be known for C-MMSE-PPE. Thus, in WDM configuration, Correlation and SF-MMSE-PPE can successfully estimate longitudinal power profiles, but C-MMSE-PPE may fail even in ideal simulation conditions. SF-MMSE-PPE corrected additional nonlinear rotation of about 0.37 radian caused by copropagating neighboring channels when option (2) is chosen. But this angle is not easy to estimate in WDM configuration for C-MMSE-PPE.

III. Experimental Results with WDM Transmission

Experimental setup for WDM transmission is shown in Fig. 3. Nyquist pulse shaped 96 Gbaud DP-16QAM is transmitted over 5 spans of 80 km SMF with 100 GHz spaced 44 channels of shaped ASE noise. Variable optical attenuators are inserted to simulate anomaly loss in optical transmission link. The received OSNR is set as 30 dB. Arbitrary waveform generator is used for center channel. Digital storage scope is used with coherent detection. Stored data is off-line processed for PPE. Training and pilot symbols are added for adaptive equalizer and CPR. One sample per symbol is saved for PPE. Reference waveform at the receiver is obtained by applying chromatic dispersion of transmission link after upsampling with zero padding in frequency domain. The waveform at transmitter is reconstructed based on the symbols detected by hard decision. The total number of 40 waveforms with 722400 symbols are processed and averaged over the number of waveforms to find longitudinal power profile.

Fig. 4(a) shows the PPE results when launch power is set as 4.8 dBm per channel. SF-MMSE-PPE shows estimated

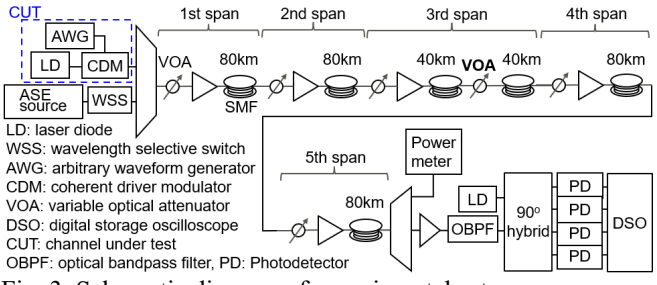

Fig. 3. Schematic diagram of experimental setup.

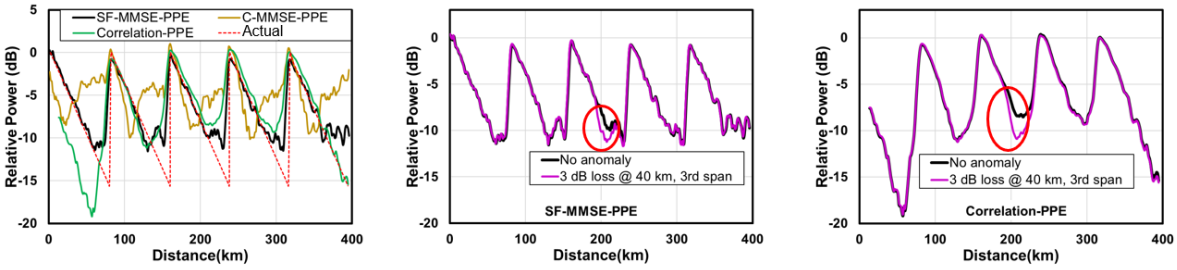

(a) (b) (c)

Fig. 4. (a) Estimated longitudinal power profile depending on PPE methods, (b) anomaly detection by SF-MMSE-PPE, (c) anomaly detection by Correlation-PPE.

power profile close to the theoretical estimation except the region where signal power is low in fiber. The minor discrepancy might be due to small nonlinear interference noise and XPM from neighboring channels. Correlation-PPE also estimates power profile because it does not need to know nonlinear rotation of constellation, but the intensity profile shows some offset for the first span. But C-MMSE-PPE could not estimate power profile at all due to unknown nonlinear rotation of constellation. Fig. 4(b) and (c) show the estimated longitudinal power profile with or without anomaly loss of 3 dB added at 40 km of the third span. Both PPEs show good agreement between reference profiles (without anomaly loss) and probed profiles (with anomaly) except the location of anomaly loss (marked with red circles), which makes both PPEs are good for anomaly detection in optical transmission links.

IV. Optical Network Tomography Tool

Prototype of optical network tomography is demonstrated, and the detail test bed information can be found in [9]. Figure 5 (a) shows the GUI of the prototype where network topology, path information, network usage, and monitoring options are shown. Fig. 5 (b) shows GUI for the detected anomaly and analysis of the anomaly when it is located at 20 km of the 3rd span or 180 km from the transmitter. Fig. 5 (c) shows another capability of the tool that can identify optical fibers. Longitudinal power profile is plotted with respect to accumulated dispersion along the transmission line of 9 spans consisted with two different fiber types. Each span length is known such that correct fiber type can be identified based on dispersion of each span. In this example, NZDSF in the 6th span is identified and the rest spans are SMF.

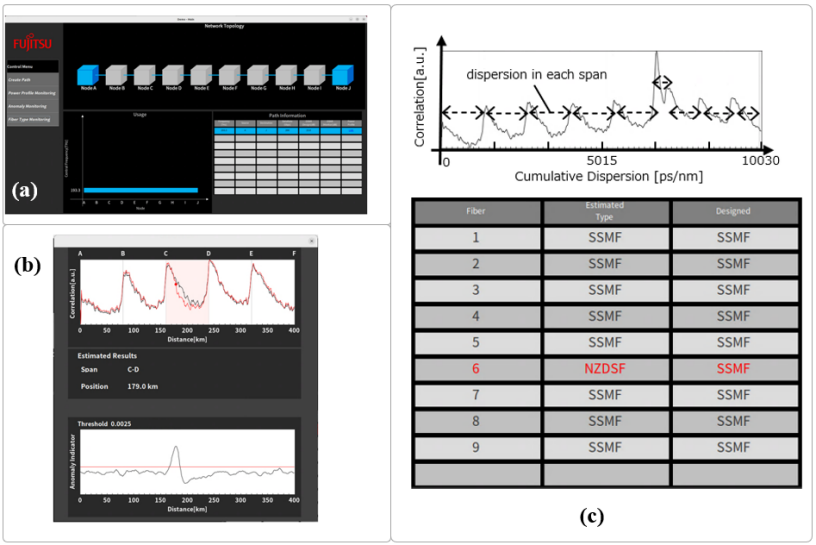

Fiber	Estimated Type	Designed
1	SSMF	SSMF
2	SSMF	SSMF
3	SSMF	SSMF
4	SSMF	SSMF
5	SSMF	SSMF
6	NZDSF	SSMF
7	SSMF	SSMF
8	SSMF	SSMF
9	SSMF	SSMF

(c)

Fig. 5. (a) GUI for prototype optical network tomography, (b) GUI for anomaly detection, (c) fiber type identification of mixed fiber transmission links.

V. Conclusion

Longitudinal power profile estimation based on coherent optical receiver is very attractive solution for optical link monitoring to enable autonomous and disaggregated optical networks. We showed that SF-MMSE-PPE and Correlation-PPE can work for WDM transmission configurations while C-MMSE-PPE may fail, even in ideal simulation study where nonlinear rotation of constellation may not be known due to copropagating channels. We also reviewed prototype of optical tomography networks that can analyze anomaly in optical transmission links and identify optical fiber types in mixed fiber transmission links.

VI. Acknowledgements

This work was partly supported by the New Energy and Industrial Technology Development Organization (NEDO),Japan, project, JPNP20017 and by the National Institute of Information and Communications Technology (NICT), Japan, Grant Number 20501.

References

[1] T. Tanimura *et al.*, "Experimental Demonstration of a Coherent Receiver that Visualizes Longitudinal Signal Power Profile over Multiple Spans out of Its Incoming Signal," in Proc. of ECOC 2019, PD3.4, (2019).

[2] T. Sasai *et al.*, "Revealing Raman-amplified Power Profile and Raman Gain Spectra with Digital Backpropagation," in Proc. of OFC 2021, M3I.5, (2021).

[3] T. Sasai *et al.*, "Digital Longitudinal Monitoring of Optical Fiber Communication Link," J. Light. Tech., vol. 40, no. 8, pp. 2390-2408, 2022.

[4] S. Gleb *et al.*, "Fiber link anomaly detection and estimation based on signal nonlinearity," in Proc. of ECOC 2021, Tu2C2.5, (2021).

[5] M. Eto *et al.*, "Location-resolved PDL Monitoring with Rx-side Digital Signal Processing in Multi-span Optical Transmission System," in Proc. of OFC 2022, Th1C.2, (2022).

[6] T. Sasai *et al.*, "Proposal of Linear Least Squares for Fiber-Nonlinearity-Based Longitudinal Power Monitoring in Multi-Span Link," in Proc. of OECC 2022, WB3-1, (2022).

[7] T. Sasai, "Digital Longitudinal Monitoring of Optical Transmission Link," in Proc. of ECOC 2022, Th1D.1, (2022).

[8] I. Kim *et al.*, "Robust Longitudinal Power Profile Estimation in Optical Networks using MMSE with Complex Scaling Factor," in Proc. of OFC 2023, W4H.6, (2023).

[9] R. Shinzaki *et al.*, "Optical Network Tomography: Demonstration of Anomaly Loss Monitoring and Fiber-Type Identification," in Proc. of OFC 2023, M3Z.2, (2023).